Reversible Surface Aggregation in Pore Formation by Pardaxin

Doron Rapaport,* Ruth Peled,‡ Shlomo Nir,‡ and Yechiel Shai*
*Department of Membrane Research and Biophysics, The Weizmann Institute of Science, and ‡Seagram Center for Soil and Water Science, Faculty of Agriculture, The Hebrew University of Jerusalem, Rehovot 76100, Israel

ABSTRACT The mechanism of leakage induced by surface active peptides is not yet fully understood. To gain insight into the molecular events underlying this process, the leakage induced by the peptide pardaxin from phosphatidylcholine/phosphatidylserine/cholesterol large unilamellar vesicles was studied by monitoring the rate and extent of dye release and by theoretical modeling. The leakage occurred by an all-or-none mechanism: vesicles either leaked or retained all of their contents. We further developed a mathematical model that includes the assumption that certain peptides become incorporated into the vesicle bilayer and aggregate to form a pore. The current experimental results can be explained by the model only if the surface aggregation of the peptide is reversible. Considering this reversibility, the model can explain the final extents of calcein leakage for lipid/peptide ratios of >2000:1 to 25:1 by assuming that only a fraction of the bound peptide forms pores consisting of $M = 6 \pm 3$ peptides. Interestingly, less leakage occurred at 43°C than at 30°C, although peptide partitioning into the bilayer was enhanced upon elevation of the temperature. We deduced that the increased leakage at 30°C was due to an increase in the extent of reversible surface aggregation at the lower temperature. Experiments employing fluorescein-labeled pardaxin demonstrated reversible aggregation of the peptide in suspension and within the membrane, and exchange of the peptide between liposomes. In summary, our experimental and theoretical results support reversible surface aggregation as the mechanism of pore formation by pardaxin.

INTRODUCTION

Pore formation and leakage occur in cells upon addition of toxic polypeptides to the medium (Primor et al., 1978; Harshman et al., 1989; Wu and Aronson, 1992; Gazit and Shai, 1993; Ghosh et al., 1993; Shai, 1994) or during interactions of certain viruses with liposomes and cells (Spruce et al., 1989; Cheetham et al., 1990; White, 1992). A better understanding of pore formation and leakage may be helpful in optimizing drug delivery via liposomes, because the leakage induced by serum components may occur in certain cases by pore formation. Studies on the kinetics of leakage and channel formation by peptides from various sources have been reported (Lear et al., 1988; Schwarz and Beschiaschvili, 1989; Rafalski et al., 1991; Martin et al., 1991; Düzgünes and Shavnin, 1992; Epand et al., 1992).

Leakage from liposomes due to pore formation by peptides can be characterized by the following (Parente et al., 1990): 1) The extent of leakage increases with time until it reaches its final extent, which is dependent on the lipid/peptide ratio. 2) The leakage of vesicle contents follows an all-or-none mechanism (Weinstein et al., 1981), i.e., when the entrapped molecules are small enough to be released, some of the vesicles release all of their contents, whereas others retain all their contents. The leakage induced by several peptides, among them the model peptide GALA (Parente et al., 1990), the fusion peptide of human immunodeficiency virus (HIV) (Nieva et al., 1994), and the amphipathic peptide pardaxin (Rapaport et al., 1994), fulfills these requirements and therefore may occur via pore formation.

The mathematical model of pore formation includes the assumption that after a rapid stage of peptide binding to the vesicle membranes, surface aggregation of peptide occurs. When the structure and conformation of the peptide used are appropriate, the aggregates that have reached a critical size (i.e., include M or more peptides) will form a pore. If surface aggregation of the peptide is irreversible, then vesicles that include M or more bound peptides will eventually leak all of their encapsulated contents (criterion 2), whereas the other vesicles will not leak at all. The kinetics of leakage is dictated by the kinetics of surface aggregation, because once a pore has formed, the leakage of all the contents occurs within less than 1 s (Lewis and McConnel, 1978; Parente et al., 1990), thus yielding a finite final extent (criterion 1). The size of the pore determines the size of molecules that can leak (criterion 2) and the final extent of leakage. The model correctly simulated the kinetics of leakage and in addition yielded quantitative predictions of the increase in the final extent of leakage with an increase in the sizes of the liposomes (Parente et al., 1990).

Pardaxin is an amphipathic 33-residue neurotoxic peptide with the sequence GFFALIPKIISSPLFKTLLSAVGSALSSSGGQE. It was found to interact with various lipid vesicles and to induce the leakage of entrapped dyes (Lazarovici et al., 1986; Shai et al., 1988, 1990, 1991; Rapaport et al., 1994). Moreover, using fluorescently labeled analogs, we have shown that pardaxin tends to self-associate in its membrane-bound state (Rapaport and Shai, 1991, 1992). The model that includes the assumption of irreversible

Received for publication and in final form

Address reprint requests to Dr. Yechiel Shai, Department of Membrane Research and Biophysics, The Weizmann Institute of Science, Rehovot 76100, Israel. Tel.: 972-89-342711; Fax: 972-89-344112; E-mail: bmshai@weizmann.weizmann.ac.il.

0006-3495/96/06/2502/11 $2.00

surface aggregation was found to be inappropriate for describing pardaxin-induced leakage, and therefore, in the current study, we extended the model by considering reversible surface aggregation of the peptide. When surface aggregation is reversible, only a fraction of the vesicles containing more than M peptides will include a pore and leak all of their contents. We experimentally confirmed our deduction of reversible surface aggregation of pardaxin in membranes composed of PC/PS/Chol by studying the effect of temperature on the leakage and by employing fluorescently labeled peptide.

MATERIALS AND METHODS

Materials

Egg phosphatidylcholine (PC) and phosphatidylserine (PS) from bovine spinal cord (sodium salt, grade I) were purchased from Lipid Products (South Nutfield, England). Cholesterol (extra pure) was purchased from Merck (Darmstadt, Germany) and was recrystallized twice from ethanol. *N*-(7-Nitrobenz-2-oxa-1, 3-diazol-4-yl) (NBD)-fluoride, calcein, and reagents for peptide synthesis were obtained from Sigma. *N*-(Lissamine-rhodamine B sulfonyl) phosphatidylethanolamine (Rh-PE), *N*-(7-nitrobenz-2-oxa-1,3-diazol-4-yl)phosphatidylethanolamine (NBD-PE), and 5-(and 6)-carboxyfluorescein, succinimidyl ester were purchased from Molecular Probes (Junction City, OR).

Peptide synthesis, modification, and purification

The peptide pardaxin was synthesized and labeled at its N-terminus as previously described (Merrifield et al., 1982; Shai et al., 1990; Rapaport and Shai, 1992). Briefly, resin-bound peptide was treated with trifluoroacetic acid to remove the *t*-butyloxycarbonyl protecting group from its N-terminal amino group. The peptide was then reacted with either 5- (and 6-) carboxyfluorescein, succinimidyl ester, or NBD-fluoride and finally cleaved from the resins by HF. The peptides were purified (>95% homogeneity) by reverse-phase high-performance liquid chromatography on a C_{18} column using a linear gradient that increased from 25% to 80% acetonitrile in 0.1% trifluoroacetic acid in 40 min. The composition and mass of the peptide were verified by amino acid analysis and fast atomic bombardment mass spectrometry, respectively.

Preparation of lipid vesicles

Large unilamellar vesicles (LUVs) were prepared from phospholipids by extrusion (Hope et al., 1985). Dry lipids were hydrated in buffer and dispersed by vortexing to produce multilamellar vesicles. The lipid suspension was frozen and thawed five times and extruded three times through 0.4-μm-pore-diameter polycarbonate membranes followed by eight extrusions through 0.1-μm-pore-diameter membranes (Poretics Corp., Livermore, CA). The lipid concentrations of the liposome suspensions were determined by phosphorus analysis (Rouser et al., 1966).

Determination of size distribution of vesicles by dynamic light scattering

Dynamic light scattering of solutions of liposomes was measured. The system used was based on a correlator made by Brookhaven Instruments BI 2030 and combined with the Contin method for data analysis.

Binding experiments

The degree of peptide association with lipid vesicles was measured by adding lipid vesicles to 0.1 μM NBD-labeled peptides, as previously described (Rapaport and Shai, 1991). The fluorescence intensity was measured as a function of the lipid/peptide molar ratio, with the excitation set at 467 nm (5-nm slit). The fluorescence values were corrected by taking into account the dilution factor corresponding to the addition of microliter amounts of liposomes, and by subtracting the corresponding blank (buffer with the same amounts of vesicles).

Peptide-induced lipid mixing

Lipid mixing of LUVs was measured using a fluorescent probe dilution assay, based on resonance energy transfer measurements (Struck et al., 1981). Lipid vesicles containing 0.6 mol% each of NBD-PE (energy donor) and Rh-PE (energy acceptor) were prepared in 100 mM NaCl, 25 mM HEPES, at pH 7.3, and a 1:4 mixture of labeled and unlabeled vesicles was suspended in 400 μl of the buffer at room temperature. The increase in NBD fluorescence at 530 nm, with the excitation wavelength set at 460 nm, was monitored with a Perkin-Elmer LS-50B spectrofluorometer. The fluorescence intensity before the addition of the peptide and the fluorescence intensity after the addition of Triton X-100 0.25% (v/v) were referred to, respectively, as 0 and 100% lipid mixing.

Turbidity measurements

Changes in the size distribution and state of aggregation of the vesicles were monitored by absorbance measurements. Aliquots of peptide stock solutions were added to 1-ml suspensions of 91 μM PS LUVs in buffer composed of 100 mM NaCl and 25 mM HEPES (pH 7.3). The absorbance at 405 nm was monitored continuously with a Milton Roy spectrometer.

Leakage assay

The fluorescence of calcein (MW = 623) encapsulated in liposomes at a self-quenching concentration increases when it leaks out of the vesicles because of its dilution (Allen and Cleland, 1980). Calcein-containing vesicles composed of PC/PS/cholesterol (4/4/1, w/w/w) were prepared in 60 mM calcein at pH 7.4 (10 mM HEPES). To remove unencapsulated dye, the vesicles were passed through a Sephadex G-75 column and eluted with 150 mM NaCl and 10 mM HEPES (pH 7.4). The increase in calcein fluorescence at 520 nm, with the excitation wavelength set at 490 nm, was monitored with a Perkin-Elmer LS-50B spectrofluorometer. The contribution of light scattering to the spectrum was minimized by exciting the sample with vertically polarized light and measuring horizontally polarized emitted light. The fluorescence of the liposomes alone or after the addition of Triton X-100 (final concentration, 0.5% v/v) corresponds to 0 or 100% leakage, respectively. Thus, the percentage of fluorescence recovery is defined as

$$F_t = [(I_t - I_o)/(I_{max} - I_o)] \times 100,$$

where I_o is the initial fluorescence, I_t is the fluorescence observed at time t after adding the peptide, and I_{max} is the fluorescence after the addition of Triton.

Surface aggregation

Aggregation of the fluorescein-labeled peptide results in close proximity of the probes on different molecules, and thus their fluorescence is self-quenched. Therefore, changes in the fluorescence intensity of fluorescein-labeled pardaxin were measured in the presence of various concentrations of PC/PS/Chol vesicles and native peptide. The fluorescence intensity was measured at 525 nm (5-nm slit) with the excitation set at 480 nm (5-nm

slit), on a Perkin-Elmer LS-50B spectrofluorometer. The contribution of light scattering to the spectrum was minimized by exciting the sample with vertically polarized light and measuring horizontally polarized emitted light, and by placing a cutoff filter of 515 nm between the sample and the emission detector.

Theoretical analysis of leakage due to pore formation

The model assumes that 1) the peptides bind and become incorporated into the bilayer of the vesicles and 2) peptide aggregation occurs within the membranes. When an aggregate within a membrane has reached a critical size, i.e., it consists of M peptides, a channel or pore is created within the membrane, and leakage of encapsulated molecules can occur. The size of the pore dictates the upper bound on the size (and shape) of molecules that can leak. The size of the pore depends on the number of peptides forming it.

As in a previous study (Parente et al., 1990), we assume that the process of peptide incorporation into the vesicle membranes is rapid and that once a pore has been formed in a vesicle all of its contents will leak rather quickly. Thus, the rate of leakage is assumed to be limited by the rate of formation of aggregates consisting of M or more peptides in the membrane. The kinetics of irreversible aggregation was first investigated by Smoluchowski (1917) and later extended to reversible aggregation by Blatz and Tobolsky (1945). The general scheme as treated by Bentz and Nir (1981) and Nir et al. (1983) is

$$X_1 + X_1 \underset{D_{11}}{\overset{C_{11}}{\leftrightarrow}} X_2$$
$$X_i + X_j \underset{D_{ij}}{\overset{C_{ij}}{\leftrightarrow}} X_{i+j}, \qquad (1)$$

where X_i are molar concentrations of aggregates of order i. Here we have used the same scheme, but in our case X_i denotes surface concentrations.

Previous treatments of the pore model (Parente et al., 1990; Fattal et al., 1994; Nieva et al., 1994) ignored the possibility of aggregate dissociation, setting $D_{ij} = 0$. Here, reversibility of surface aggregation of pardaxin has been considered. To facilitate the computational procedure and to avoid the use of many parameters, we have employed the same simplifications made by Smoluchowski (1917) and by Blatz and Tobolsky (1945), i.e., that $C_{ij} = C$ and $D_{ij} = D$ for all i and j. It has been shown (Peled et al., 1995) that with these assumptions the analytic solution of Blatz and Tobolsky (1945) yields results that are essentially similar to the numeric solutions (Bentz and Nir, 1981; Nir et al., 1983).

The fraction of encapsulated material that has leaked at time t is denoted by $L(t)$. Because of the dependence of the encapsulated volume on the third power of the inner diameter, a small fraction of large vesicles can contribute significantly to $L(t)$. Therefore, in the current treatment, we considered the vesicles to consist of $j = 1, \ldots S$ size classes. The distribution of vesicles according to their diameters was determined by dynamic light scattering. In practice, we set $S = 15$ and we denote the fraction of encapsulated volume in vesicles of type j by f_j, $1 \le j \le 15$.

Let A_{ij} be the normalized fraction of vesicles of size class j that contain i bound peptides, i.e.,

$$\sum_{i=0}^{N_j} A_{ij} = 1, \qquad (2)$$

in which N_j is the largest number of peptides that can bind to a vesicle of size class j. The procedures for calculating the quantities A_{ij} from binding data have been described before (Nir et al., 1986; Bentz et al., 1988; Parente et al., 1990; Nir et al., 1994). The expression for $L(t)$ is given by

$$L(t) = \sum_{j=1}^{S} \sum_{i=M}^{N_j} Z(M, t, i, j, C, D) A_{ij} f_j, \qquad (3)$$

in which $Z(M,t,i,j,C,D)$ is the probability that at time t a vesicle of size class j that contains i bound peptides will include an aggregate consisting of M or more peptides, and C and D are the rates of surface aggregation and disaggregation, respectively. The function $Z(M,t,i,j,C,D)$ is described in the Appendix.

The final extents of leakage are obtained by setting $t = \infty$. Experimentally, final extents of leakage were considered at $t = 900$ s. Because the functions A_{ij} and f_j are fixed quantities, the final extents of leakage depend only on the value of M, the pore size, and the equilibrium constant for two-dimensional aggregation,

$$K_s = C/D. \qquad (4)$$

The parameters M and K_s are determined from the final extents of leakage for a wide range of lipid/peptide ratios.

RESULTS AND DISCUSSION

Our focus has been on the analysis of the extent of peptide-induced leakage and elucidation of the mode of peptide aggregation in the membrane. The leakage experiments were conducted at lipid/peptide ratios that varied from 2600:1 to 25:1. First we verified that under these conditions pardaxin is not able to induce vesicle aggregation or fusion to a significant extent. A control experiment that applied a fluorescence resonance energy transfer assay (Struck et al., 1981) after lipid mixing was performed. At lipid/peptide ratios of 221:1 and 84:1 we found that vesicle fusion did not occur, because no membrane mixing, reflected by an increase in fluorescence, was observed (results not shown). Turbidity measurements at a lipid concentration similar to that used in the leakage assay (32 μM) indicated that peptide-induced vesicle aggregation did not occur at lipid/peptide ratios of 138:1, 64:1, and 53:1 (data not shown). Therefore, the observed peptide-induced leakage occurred from each vesicle essentially independently of its interaction with other vesicles.

Binding experiments

The analysis of the leakage results and the determination of the pore size are based on knowledge of the amount of peptide bound to the liposomes in the range of lipid/peptide ratios used in the leakage experiments. These values are necessary to calculate the elements of the distribution function A_{ij} in Eq. 2. Therefore, we measured the binding of the peptide to vesicles utilizing the fluorophore NBD, as its fluorescence intensity reflects the environment in which the probe is located (Frey and Tamm, 1990; Rapaport and Shai, 1991). NBD-labeled pardaxin (0.1 μM), in buffer composed of 150 mM NaCl and 10 mM HEPES (pH 7.4), was titrated with PC/PS/Chol (4/4/1, w/w/w) vesicles, and the increases in the fluorescence intensities due to peptide membrane partition were recorded at 25°C and 43°C.

A value for F_∞, the fluorescence signal obtained when all of the peptide is bound to lipid, was extrapolated from a double-reciprocal plot of F (total peptide fluorescence) versus C_L (total concentration of lipid), as previously described (Schwarz et al., 1986). This value enabled us to determine the fraction of membrane-bound peptide at each lipid concentration for both temperatures, and the results are shown in Fig. 1. From the results it is evident that at each lipid-to-peptide ratio, the elevated temperature facilitates the partitioning of higher amounts of peptide into the liposomal membranes. We analyzed the data as a partition equilibrium (for details see Rapaport and Shai, 1991) using the formula

$$X_b = K_p C_f,$$

where X_b is defined as the molar ratio of bound peptide per 60% of the total lipid, K_p corresponds to the partition coefficient, and C_f represents the equilibrium concentration of free peptide in the solution. The surface partition coefficients of pardaxin were calculated to be 1.0 ($\pm$0.3) $\times$ 10^5 M^{-1} and 3.4 ($\pm$0.3) $\times$ 10^5 M^{-1} at 25°C and 43°C, respectively.

Final extents of leakage

The leakage of calcein was monitored by the dequenching of its fluorescence due to its dilution. The mechanism of leakage was determined at 43°C. When 64% leakage was observed, the vesicle suspension was taken from the cuvette and eluted through a gel filtration column. It was found that whereas initially the fluorescence of the dye within the vesicles was 90% quenched, the dye within the eluted vesicles after the leakage experiments was 84% quenched. According to a mechanism of graded release, the expected value was 45% (Matsuzaki et al., 1993). Hence, we can conclude that the leakage occurred essentially according to an all-or-none mechanism, which is indicative of a leakage mechanism by pore formation.

Fig. 2 shows the extents of calcein leakage from the liposomes at 30°C and at 43°C 15 min after the addition of pardaxin at lipid/peptide ratios ranging from 2600:1 to 25:1. The presentation of the data as a function of bound peptide/lipid ratios emphasizes the fact that for the same amount of bound peptide, a greater leakage occurs at 30°C than at 43°C. We denote the leakage level attained after 15 min as the "final extent," but unlike the leakage induced by other peptides, e.g., GALA (Parente et al., 1990), the leakage induced by pardaxin still proceeded after 15 min, although at an extremely slow rate.

Analysis of final extents of leakage: pore formation by reversible surface aggregation

Because, as $t \rightarrow \infty$, Z becomes a function of K_s (see Eq. 3), the final extent of leakage becomes

$$L_\infty = \sum_{j=1}^{s} \sum_{i=M}^{N_j} Z(M, \infty, i, j, K_s) A_{i,j} f_j \quad (5)$$

for reversible aggregation, whereas

$$L_\infty = \sum_{j=1}^{s} \sum_{i=M}^{N_j} A_{i,j} f_j \quad (6)$$

for irreversible aggregation (Parente et al., 1990). Equation 6 reflects the assumption that when aggregation is irrevers-

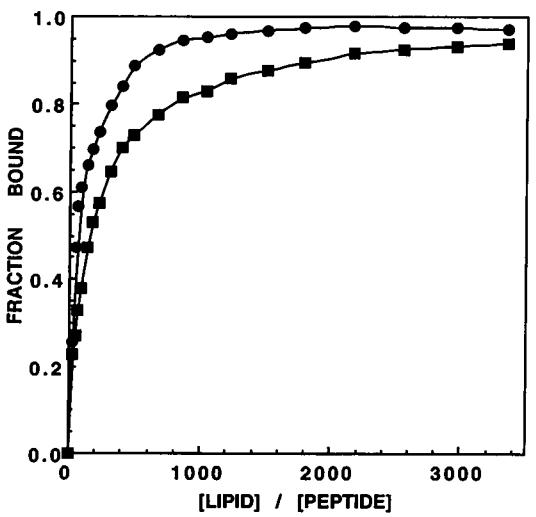

FIGURE 1 Effect of temperature on the binding of NBD-labeled pardaxin to lipid vesicles. Peptide (0.1 μM) was titrated with PC/PS/Chol (4:4:1) small unilamellar vesicles, in buffer composed of 100 mM NaCl, 25 mM HEPES, pH 7.3, at either 43°C (●) or 25°C (■). The increase of fluorescence intensity was monitored with the excitation at 460 nm and the emission at 530 nm. The fraction of bound peptide was calculated as described in the text.

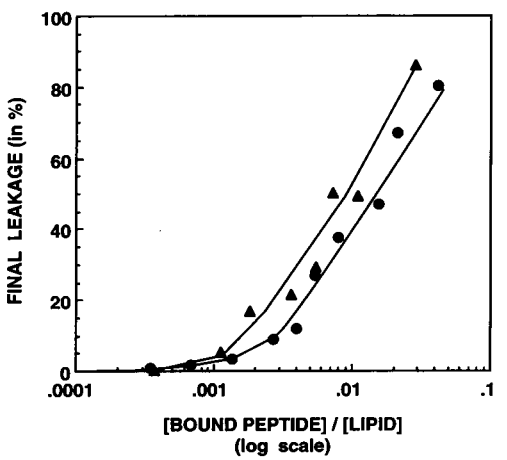

FIGURE 2 Calcein release induced by pardaxin as a function of bound peptide/lipid molar ratio. Pardaxin at various amounts was added to vesicles containing 60 mM encapsulted calcein at either 43°C (●) or 30°C (▲). The leakage of calcein after 15 min was monitored fluorometrically (see text) and is plotted as a function of the bound peptide/lipid ratio. The bound peptide was calculated according to the partition coefficients obtained from the binding experiments.

ible, all of the peptides within a membrane will eventually be incorporated into a single aggregate, so that all vesicles with at least M bound peptides will eventually leak.

We have compared the predictions of Eqs. 5 and 6 in an attempt to explain the final extents of leakage as a function of lipid/peptide ratio. Table 1 presents the experimental values of the final extents of leakage for several lipid/peptide ratios and the pore sizes, M, which were deduced from them using Eq. 6. The table shows that when the surface aggregation of pardaxin is assumed to be irreversible, the derived M values vary between ~120 and several thousand. In view of the large deduced values of M and their variability with lipid/peptide ratios, this model is unacceptable. Setting the rate of aggregate dissociation, $D = 0$ implies that $K_s = C/D$ tends to infinity. The probability of finding large surface aggregates of the peptide diminishes with decreasing K_s values. Consequently, a decrease in K_s corresponds to smaller deduced values of M for each value of the lipid/peptide ratio (see Eq. 5).

In Table 1, we present the values of M deduced from Eq. 5 using different values of K_s. The best fit at 30°C is obtained with $K_s = 0.002$ and $M = 6$. The limits of the fit were $M = 6 \pm 3$, with corresponding K_s values of 0.0002 for $M = 3$ and 0.005 for $M = 9$. The predicted final extents of leakage for the values $K_s = 0.002$ and $M = 6$ are also presented and compared to the experimental values. To fit the experimental values of the final extents of leakage at 43°C, we used the same value of M, but K_s was set at 0.001. The results in Table 1 indicate a very good fit of calculated values to the experimental values of final extents. The values of R^2 were 0.94 and 0.98 at 30°C and 43°C, respectively. The corresponding values of root mean square error (RMSE) were 6.9% and 4.2%, i.e., within the estimated experimental errors. The RMSE is given by

$$\mathrm{RMSE} = \left[\sum_{i=1}^{n} (Y_i - Y_{ci})^2/(n-2)\right]^{1/2}, \qquad (7)$$

in which Y_i and Y_{ci} are experimental and calculated values of percentage leakage and n is the number of data points.

Kinetics of calcein leakage

The experimental kinetics of calcein leakage from the liposomes are shown in Fig. 3. The effect of temperature on the kinetics of leakage is shown by comparing the results at 30°C (Fig. 3 *A*) with those at 43°C (Fig. 3 *B*) for the same lipid/peptide ratio. It is evident that the kinetics of calcein release is enhanced with the increase in temperature, whereas the final extent is decreased with the increase in temperature (Fig. 1).

TABLE 1 Final extents of leakage and minimum number of peptides for pore formation

Temp. (°C)	Lipid:peptide molar ratio*	Experimental leak (%)‡	Calculated leak (%)	M for different values of K_s			
			$M = 6$, $K_s = 0.002$	K_s = inf.	$K_s = 0.02$	$K_s = 0.002$	$K_s = 0.0002$
30	2210	0.0	0.5	119	20	8	3
	737	3.5	5.9	279	18	6	3
	442	16.5	13.0	376	16	6	3
	221	24.5	27.9	680	19	6	3
	147	28.5	38.4	942	21	7	3
	111	50.5	46.1	954	16	6	2
	74	49.0	56.5	1526	20	7	3
	28	86.0	76.8	2267	13	4	2
			$M = 6$, $K_s = 0.001$	K_s = inf.	$K_s = 0.01$	$K_s = 0.001$	$K_s = 0.0001$
43	2654	1	0	118	11	4	3
	1380	2	1	216	14	5	3
	1150	1	1	268	18	6	3
	676	4	3	419	17	6	3
	466	4	7	609	20	7	3
	342	10	11	723	18	6	3
	233	12	17	1036	20	7	3
	171	27	24	1097	17	6	3
	117	27	34	1598	20	7	3
	114	37	34	1439	17	6	2
	86	36	42	2052	20	7	3
	59	47	52	2617	19	7	3
	43	59	60	3055	18	6	2
	30	64	68	3974	20	7	3
	22	80	74	4388	15	5	2

The critical number of peptides required for pore formation, M, was calculated for each lipid/peptide ratio with different values of K_s to fit the experimental values of final extent. Using the best fit for M, $M = 6$, the experimental final extents are compared to a calculated value using Eq. 5.

*The experimental error is ±15%.

‡The experimental error is ±5%.

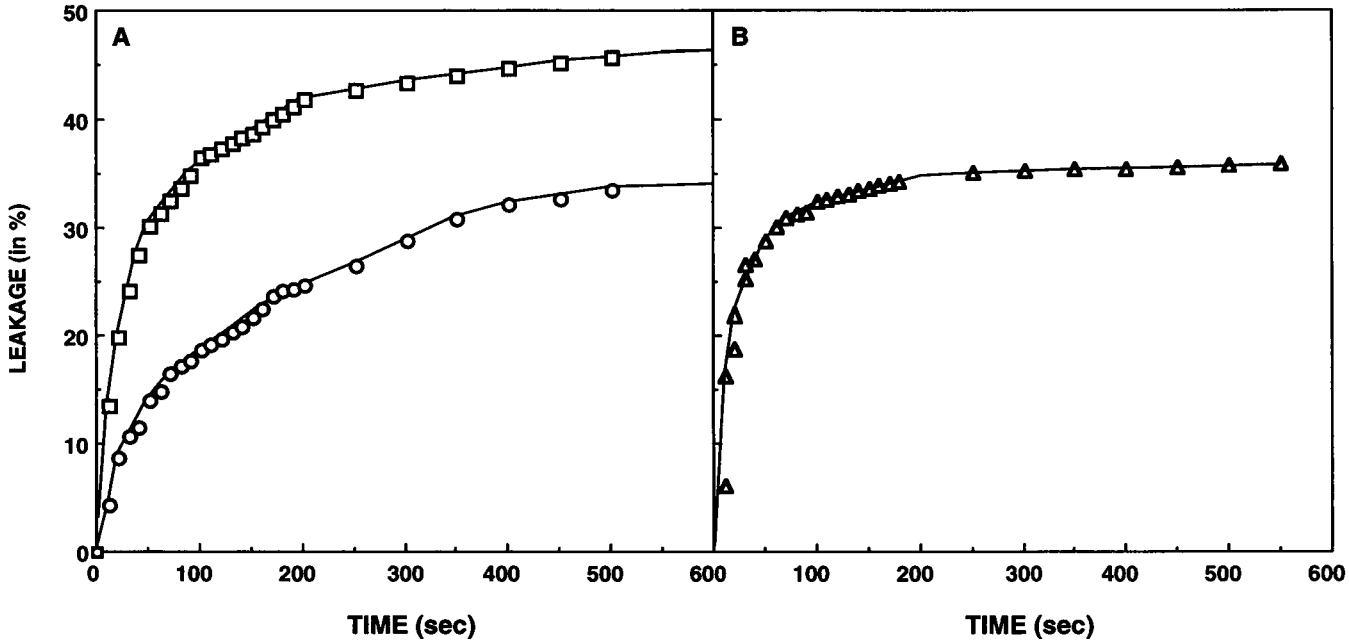

FIGURE 3 Experimental kinetics of calcein release induced by pardaxin. Various amounts of pardaxin were added to vesicles containing 60 mM encapsulted calcein at 30°C (*A*) or 43°C (*B*). The kinetics of the leakage were followed by monitoring the increase of the fluorescence intensity at 520 nm and are plotted versus time. For each amount of added peptide the molar ratio of bound peptide/lipid was calculated, and the experimental kinetics are plotted. Lipid/peptide molar ratios: □, 110; ○, 221 (*A*); △, 114 (*B*).

Reversibility of binding and surface aggregation

Our theoretical analysis supports a mechanism of calcein leakage by pore formation after reversible surface aggregation of the peptide pardaxin. In the following, we present the results of experiments that demonstrate that binding of the peptide to PC/PS/Chol liposomes and its aggregation, both within the membrane and in solution, are indeed reversible processes.

In testing whether the binding and the surface aggregation of the peptide are reversible processes, we utilized a fluorescein-labeled peptide. The fluorescence of the fluorescein probe is self-quenched because of the close proximity of other fluorophore molecules (Chen and Knutson, 1988). Therefore, the fluorescence intensity of the labeled peptide can give information on its aggregation state. The data presented in Fig. 4 (*continuous line*) revealed that the labeled peptide (0.84 μM) tends to self-associate to a limited extent and in slow kinetics in buffer composed of 150 mM NaCl and 10 mM Tris (pH 7.4). However, upon addition of PC/PS/Chol LUV (40 μM), a dramatic decrease in the fluorescence was observed, reflecting fast binding of the peptide to the vesicles and self-quenching of the probes because of their high local concentration in the membrane. A further addition of vesicles to a final concentration of 381 μM caused an increase in the fluorescence due to redistribution of the peptide among all of the vesicles. When the peptide was added in the presence of 79 μM lipid vesicles (Fig. 4, *dashed line*), the fluorescence level was higher than that observed in the presence of 40 μM, probably because of a lower peptide concentration in the bilayer. The final level after adding vesicles to a final concentration of 381 μM was similar to that in the first case. For comparison, the peptide was added initially to 381 μM lipid (*dotted line*), and the resulting fluorescence level was higher than in the first two cases. However, the fluorescence level in both cases (*continuous and dashed lines*), where a large amount of vesicles was added after a small amount, continued to increase, reflecting a slow process of redistribution of the peptide molecules among the total liposome population. Addition of detergent (Triton X-100), which solubilized the vesicles, resulted in a sharp increase in the fluorescence intensity, suggesting that the aggregated peptide was in the membrane-bound state. These results suggest that the binding of the peptide to the membrane is a reversible process.

To study the reversibility of the surface aggregation of the peptide, the ability of native peptide to reverse the self-quenching of labeled peptide was investigated. Indeed, the fluorescence level increased when a native peptide (0.84 μM) was added to 0.42 μM labeled peptide premixed with 40 μM vesicles (Fig. 5, *continuous line*). The concentrations of the labeled peptide and the vesicles were such that about 75% of dye leakage was observed (Fig. 3). A similar fluorescence level was obtained when the native peptide was first mixed with the vesicles and the labeled peptide was added later. These results demonstrate that surface aggregation of pardaxin is a dynamic and reversible process. The results of Fig. 4 might suggest that the aggregation of pardaxin in solution is also a reversible process. We have tested this possibility directly by comparing the extents of calcein leakage in two cases: in the first case the peptide is

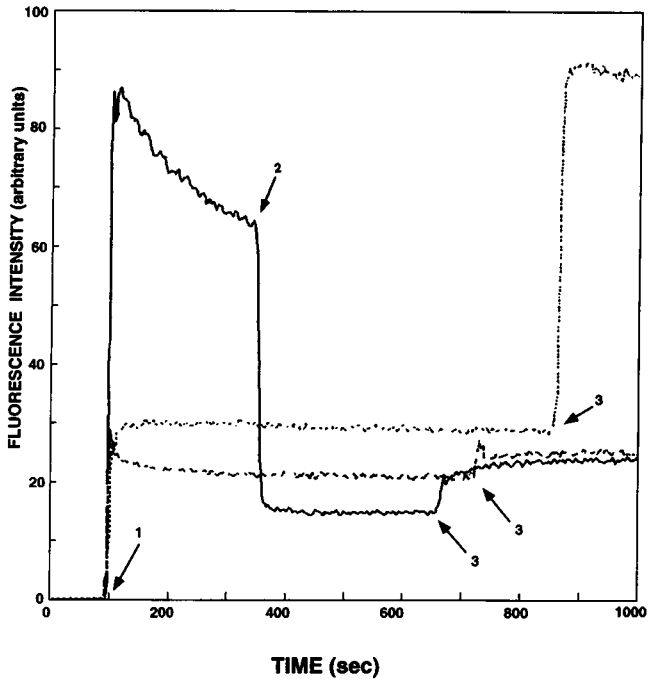

FIGURE 4 Reversible binding of fluorescein-labled pardaxin. The fluorescence intensity of the labeled peptide was monitored at 525 nm (slit 5 nm) with the excitation at 480 nm (slit 5 nm). The experiment was done in a buffer composed of NaCl (150 mM) and Tris (10 mM), pH 7.4, and LUVs composed of PC/PS/Chol 4/4/1 (w/w/w) were used. Labeled peptide (0.84 μM) was added at the first time point to buffer (——), to 381 μM vesicles (·····), or to 79 μM vesicles (– – –). Vesicles (40 μM) were added to the peptide solution at the second time point (——). At the third time point more lipids were added, at 302 μM (– – –) or 341 μM (——); thus the final lipid concentration in all cases was 381 μM. In the third case (·····) Triton X-100 (0.1% v/v) was added at point 3.

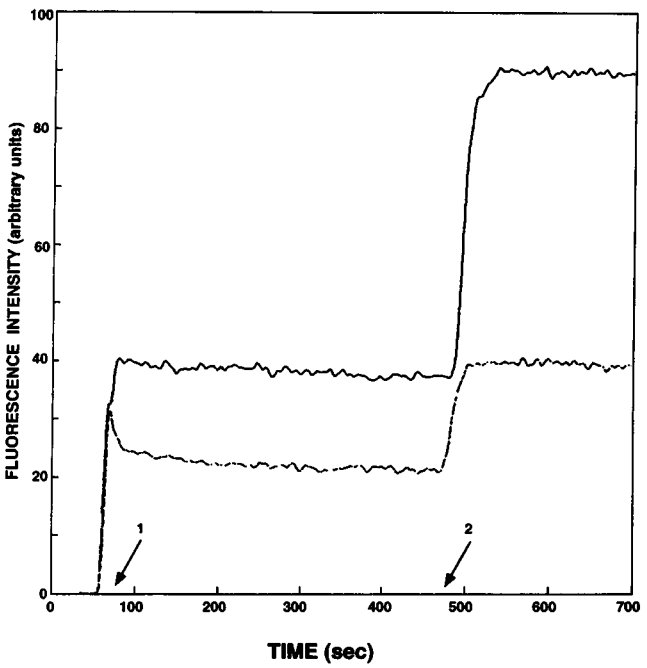

FIGURE 5 Reversibility of surface aggregation of fluorescein-labeled pardaxin. The fluorescence intensity of the labeled peptide was monitored at 525 nm (slit 5 nm) with the excitation at 480 nm (slit 5 nm). The experiment was done in a buffer composed of NaCl 150 mM and Tris 10 mM, pH 7.4, and LUVs composed of PC/PS/Chol 4/4/1 (w/w/w) were used. Labeled peptide (0.42 μM) was added at the first time point to either a suspension of lipid vesicles alone (40 μM) (– – –), or the same amount of vesicles with pre-bound native peptide (0.84 μM) (——). At the second time point native peptide (0.84 μM) was added to the first solution (– – –), and Triton X-100 (0.1% v/v) was added to the second solution (——).

added to a vesicle suspension, and in the second case the order is reversed and the peptide is incubated for a few minutes in solution before the vesicles are added. The results in Fig. 6 indicate that the leakage levels obtained in the two cases are similar, although with slightly different kinetics. Assuming that the peptide is at least partially aggregated in solution, and because the peptide is believed to bind to vesicles in the monomeric form, these results indicate reversibility of its aggregation in solution. Furthermore, in another experiment we diluted a solution of the labeled peptide sixfold. If the aggregation in solution were not reversible, then the dilution would not affect the state of quenching of the fluorescence of the peptide. However, the dilution resulted in about a twofold increase in the normalized fluorescence (results not shown).

GENERAL DISCUSSION

We demonstrated that the mechanism of pardaxin-induced leakage from PC/PS/Chol (4/4/1) LUVs is via pore formation utilizing reversible surface aggregation of the bound peptide. The evidence of formation of pores consisting of at least $M = 6 \pm 3$ peptides is based on 1) observation of final extents of leakage, 2) the finding of an all-or-none mechanism of leakage, 3) theoretical modeling that yields simulations and predictions of the final extents of leakage for a wide range of lipid/peptide ratios. The theoretical analysis utilized detailed information on peptide binding and size distribution of the liposomes, which is needed, according to Eqs. 2 and 3. Knowledge of the size distribution of liposomes is crucial, because the larger liposomes contain on average more bound peptides and are more likely than small liposomes to leak at high lipid/peptide ratios. In addition, the leakage of a large liposome contributes more to the final extent of leakage than does the leakage of a small one. This pattern differs from the tendency of large liposomes to be more stable and less permeable. Large liposomes also yielded initially slower kinetics of Ca^{2+}-induced leakage than smaller liposomes (Bentz et al., 1983; Nir et al., 1983). This predicted pattern of a larger extent of leakage from larger liposomes was shown in a previous study with pardaxin (Rapaport et al., 1994) as well as in studies employing various peptides such as GALA (Parente et al., 1990) and the fusion peptide of HIV (Nieva et al., 1994). 4) Earlier studies with many analogs of pardaxin using a variety of biophysical and functional assays, which included single-channel experiments (Shai et al., 1990, 1991; Shai, 1994), fluorescence studies (Rapaport and Shai, 1992), and

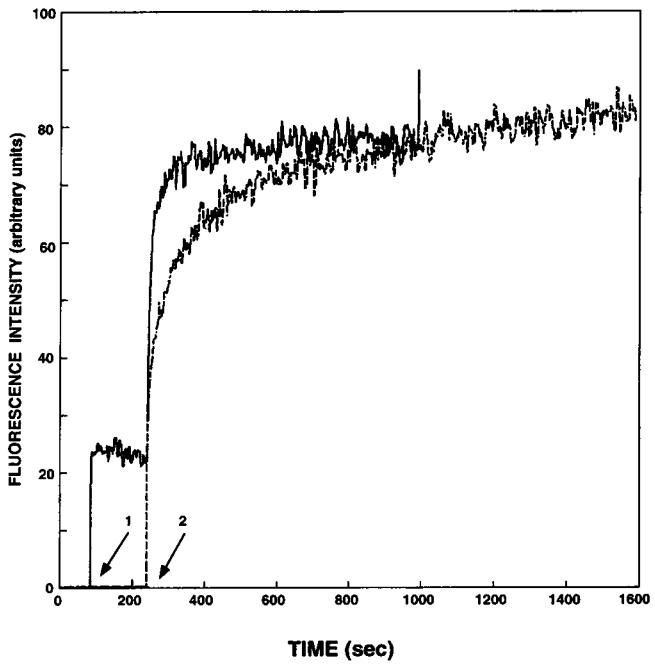

FIGURE 6 Influence of order of addition of peptide and vesicles on the extent of pardaxin-induced leakage. At the first time point 0.4 μM pardaxin (– – –) or 21 μM vesicles loaded with 60 mM calcein (——) were added to a buffer composed of NaCl (150 mM) and HEPES (10 mM), pH 7.4. Then at the second time point vesicles were added to the peptide in solution (– – –), or pardaxin was added to the vesicle suspension (——). The fluorescence intensity at 520 nm was monitored and is plotted versus time.

energy calculation modeling (Lazarovici et al., 1992), support a channel formation mechanism as the mode of action of pardaxin, rather than local disruption. In these channels four is the minimum number of pardaxin molecules required to form a conducting channel. It should also be noted that the results clearly indicate that aggregates of peptides do remain in the pool of reversible surface aggregates for times longer than required for complete leakage of calcein (Fig. 5).

Using fluorescently labeled peptides, we have demonstrated that pardaxin molecules tend to self-aggregate efficiently within lipid vesicles (Rapaport and Shai, 1991, 1992). The realization that, unlike results with the synthetic peptide GALA and the fusion peptide of HIV, the surface aggregation of pardaxin is a reversible process was first reached by analyzing the final extents of leakage. At 43°C, if the possibility of reversible surface aggregation of pardaxin were not considered, the calculations would yield very large values of M, from 120 to 4400, depending on the lipid/peptide ratio (see Table 1). Furthermore, we experimentally demonstrated the reversibility of surface aggregation of pardaxin, observed as dequenching upon the addition of unlabeled peptide to the fluorescein-labeled peptide (Fig. 5). This dequenching was due to exchange between labeled and unlabeled peptides in surface aggregates. The results also demonstrated reversibility of the aggregation of pardaxin in solution and peptide exchange between vesicles. This is different from the behavior observed with the fusion peptide of HIV, where leakage and fusion were almost completely abolished when the liposomes were added into suspension 1 min after the peptide, and where exchange of the peptide between vesicles was minimal (Nieva et al., 1994). In our case, a large extent of leakage was still observed, even when the liposomes were added to the buffer several minutes after the peptide (Fig. 6).

It might appear that there is a discrepancy between the observations of i) a limiting extent of leakage and ii) reversibility of surface aggregation of the peptide and its exchange between vesicles. The answer is that the time it takes for peptides to exchange between vesicles is several-fold larger than the time required to reach an apparent final extent of leakage. In fact, in several cases the final extents were reached after 10 min within the experimental uncertainty. In the cases examined after 25 min, the fraction leaked was less than 1% above that of 5 min. Strictly speaking, there is a very slow increase in leakage, even after 15 min, because of the exchange of peptides between vesicles. A comparison of Figs. 4 and 5 indicates that whereas the incorporation of newly added peptide molecules into existing surface aggregates takes about 1 min (Fig. 5), the exchange of peptides from vesicles at a concentration of 40 μM lipid to a large excess of added vesicles (341 μM) does not terminate within 5 min.

We have attempted to apply calculations based on reversible surface aggregation (Peled and Nir, unpublished results) to the results with GALA (Parente et al., 1990). Despite the addition of one parameter, no improvement in the fits to final extents was achieved. The leakage induced by GALA from 1-palmitoyl-2-oleoyl-*sn*-glycero-3-phosphocholine vesicles is well explained by assuming irreversibility of both binding and surface aggregation.

The effect of temperature on binding of pardaxin to PC/PS/Chol liposomes and the subsequent leakage further elucidate details of the leakage mechanism and the interactions of the peptide with the liposomes. The results in Fig. 1 show enhanced binding with temperature. This can be explained by a weakening of intermolecular interactions between membrane constituents, which facilitates the penetration of the peptide at elevated temperatures. In contrast, the fraction of virus bound to cellular surfaces increases at lower temperatures, indicating a different mechanism of binding, namely binding to receptors rather than penetration into the membrane (Düzgünes et al., 1992). The results in Fig. 2 and Table 1 show that the extent of pardaxin-induced leakage is enhanced by a reduction in temperature. This is in contrast to the increase in permeability with temperature (Papahadjopoulos et al., 1973; Szoka and Papahadjopoulos, 1980) and to the leakage of liposomes associated with membrane fusion events. Our interpretation is that at lower temperatures the extent of surface aggregation is enhanced, as in aggregation phenomena in three dimensions.

The analysis of final extents of leakage yielded a larger value for $K_s = C/D$ (Tables 1) at 30°C than at 43°C. Hence, the observed enhanced leakage at a lower temperature is a

result of an increased fraction of vesicles that contain pores, due to a larger extent of surface aggregation of pardaxin molecules at lower temperatures. Thus we find for surface aggregation of peptides a pattern of temperature dependence similar to that previously found for particle aggregation at equilibrium (Day et al., 1980; Nir et al., 1980; Bentz and Nir, 1981; Nir et al., 1983; Peled et al., 1995). This phenomenon has been explained by the increase of the constant $K = C/D$ with decreasing temperature, due to a steeper decrease of the dissociation rate constant D than of the forward rate constant of aggregation C.

The sequence of events that occurred in our experiments when pardaxin was added to liposomes is summarized in Fig. 7. These events include reversible aggregation of the peptide in solution, reversible partitioning into the membranes, reversible surface aggregation, and finally leakage. When aggregation of liposomes occurs, pardaxin is also capable of inducing membrane fusion (Rapaport et al., 1993, 1994), but we have chosen conditions in which vesicle aggregation and fusion could be ignored, at least for the larger lipid/peptide ratios used. The results described here can help elucidate the mode of action of pardaxin in vivo. Pardaxin is secreted from certain species of soles and is postulated to be defensive, because it has shark-repelling properties and is toxic to various organisms (Primor et al., 1978). The biological activities of pardaxin are probably due to its surface-active properties, as it was shown that it interacts with biological and artificial lipid membranes (Lazarovici et al., 1986; Shai et al., 1988). Furthermore, pardaxin was found to form ion channels in artificial membrane systems (Shai et al., 1990), and its ability to trigger exocytosis from cells was explained by the potential of the peptide to form pores in the cell plasma membrane (Lazarovici and Lelkes, 1992). These accumulating data, together with the results of the present study, support a hypothesis that at least part of the biological activities of pardaxin are brought about by its ability to form pores in lipid bilayers. Our present results further suggest that these pores are formed because of reversible aggregation of monomers within the membrane.

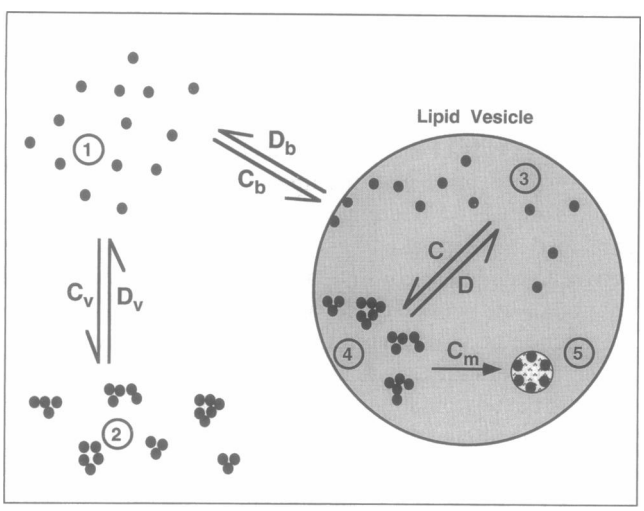

FIGURE 7 A schematic model for the processes involved in pore formation by pardaxin. (*1*) Free peptides in solution; (*2*) peptide aggregates in solution; (*3*) bound peptides in monomeric form; (*4*) aggregates of bound peptide; (*5*) pore formed by an aggregate of bound peptides. C_b and D_b are the rates of binding and dissociation of peptides to and from the membranes, respectively. C_v and D_v are the rates of aggregation and disaggregation of peptides in solution, respectively. C is the rate of aggregation of bound peptide in the membrane and D is the rate of disaggregation in the membrane. C_m is the rate of morphological change of peptide aggregates to pores. In the current treatment C_m was not considered.

Animal antibacterial peptides serve as immune substances, and they are primary defense agents (Boman, 1991; Zasloff, 1992), but the molecular events underlying their activities are still not clear, and contradicting opinions exist (Christensen et al., 1988; Steiner et al., 1988). We believe that our combined theoretical and experimental approach can be applied to other peptides to gain more insight into their modes of action.

APPENDIX: PROBABILITY OF LEAKAGE

In this section we derive an expression for $Z(M,t,i,j,C,D)$, the probability that at time t a vesicle of size j containing i bound peptides includes an aggregate of size greater than or equal to M. C and D are the rates of surface aggregation and disaggregation of the peptide, respectively. The derivation is based on those of Flory (1939) and Blatz and Tobolsky (1945), which were applied to the polymerization of organic molecules. They therefore assumed that, initially, all of the particles (monomers) are identical and that each monomer has two free ends: A and B. A polymerization reaction always involves an A end of one monomer and a B end of another. The number of unreacted A ends is thus always equal to the number of unreacted B ends and to the total number of particles (monomers plus aggregates).

Following Flory (1939), we assume that all of the monomers can be laid end to end and that each point of contact (link) is a potential bond. If we define $n(t)$ = concentration of particles (peptides in our case), monomers + aggregates; $n_0 = X_0$ = total initial concentration of monomers; then:

$$p(t) = \frac{n_0 - n(t)}{n_0}, \tag{A.1}$$

where $p(t)$ is the ratio of reacted links (bonds) to the total number of links, or the probability that a link has reacted.

Flory assumed that the reactivity of a link is independent of the number of monomers in the aggregate. Therefore the probability that a monomer chosen at random is part of an aggregate of size k is given by $k \cdot p^{k-1}(1-p)^2$, from which the relative concentration of aggregates of size k is

$$\frac{X_k}{X_0} = p^{k-1}(1-p)^2. \tag{A.2}$$

The set of reactions represented by Eq. 1 were described by Blatz and Tobolsky (1945) by the differential equations

$$\frac{dX_k}{dt} = \frac{1}{2}\sum_{i+j=k}(k_f X_i X_j - 2k_b X_{i+j}) - \sum_{i=1}^{\infty}(k_f X_i X_k - 2k_b X_{k+i}), \tag{A.3}$$

where k_f is the rate of bimolecular addition and k_b is the rate of unimolecular splitting. Summation of the Eq. A.3 gives a single differential equation in $n(t)$:

$$\frac{dn}{dt} = -\frac{1}{2}k_f n^2 + k_b(n_0 - n). \quad (A.4)$$

The solution to Eqs. A.1 and A.4 is

$$p = \frac{1}{K + \sqrt{K^2 - 1}\cdot\coth\left[\frac{1}{2}k_f n_0 t\sqrt{K^2 - 1}\right]}, \quad (A.5)$$

where

$$K \overset{\text{def}}{=} 1 + \frac{k_b}{X_0 k_f}.$$

A comparison of Eq. A.3 to similar equations (Bentz and Nir, 1981; Peled et al., 1995) yields $k_f = 2C$ and $k_b = D/2$, i.e.,

$$K \overset{\text{def}}{=} 1 + \frac{D}{4X_0 C}. \quad (A.6)$$

At equilibrium, i.e., when $t \to \infty$, $\bar{p}$ is given by

$$\bar{p} = \frac{1}{K + \sqrt{K^2 - 1}}. \quad (A.7)$$

Because K in Eq. A.6 depends on CX_0, i.e., on the size of the vesicles as well as on the number of bound peptides, this parameter must be determined for each combination of i and j. In our calculations, we follow the method used by Parente et al. (1990), i.e., we choose a reference vesicle of radius 100 nm and measure X_0 as the surface density of peptides relative to one peptide per reference area. Therefore, for a vesicle of type j with radius r_j and i bound peptides, Eq. A.6 becomes

$$K \overset{\text{def}}{=} 1 + \frac{D}{4\cdot i\cdot C}\cdot\frac{r_j^2 + (r_j - 4)^2}{100^2 + 96^2}. \quad (A.8)$$

The value of C corresponds to the outer surface of a 100-nm-radius vesicle.

The probability that a monomer chosen at random is part of an aggregate of size k is $k \cdot X_k/X_0$. Therefore, the probability that a monomer chosen at random is part of an aggregate of size greater than or equal to M is

$$\sum_{k=M}^{\infty} k\cdot p^{k-1}(1 - p)^2. \quad (A.9)$$

We assume that the probability of a vesicle leaking is equal to the above and therefore,

$$Z(M, t, i, j, C, D) = p^{M-1}(M - Mp + p), \quad (A.10)$$

where p is given by Eq. A.5 for finite time, or by Eq. A.7 for $t \to \infty$ and K is given by Eq. A.8.

We wish to thank Ms. Sue Salomon for the expert typing of the manuscript.

This work was supported in part by the Basic Research Foundation administered by the Israel Academy of Sciences and Humanities, and by the Israel Cancer Association.

REFERENCES

Allen, T. M., and L. G. Cleland. 1980. Serum-induced leakage of liposome contents. *Biochim. Biophys. Acta.* 597:418–426.

Bentz, J., and S. Nir. 1981. Mass action kinetics and equilibria of reversible aggregation. *J. Chem. Soc. Faraday Trans.* 177:1249–1275.

Bentz, J., S. Nir, and D. G. Covell. 1988. Mass action kinetics of virus-cell aggregation and fusion. *Biophys. J.* 54:449–462.

Bentz, J., S. Nir, and J. Wilschut. 1983. Mass action kinetics of vesicle aggregation and fusion. *Colloids Surf.* 6:333–363.

Blatz, P. J., and A. V. Tobolsky. 1945. Note on the kinetics of systems manifesting simultaneous polimerization- dipolimerization phenomena. *J. Phys. Chem.* 49:77–80.

Boman, H. G. 1991. Antibacterial peptides: key components needed in immunity. *Cell.* 65:205–207.

Cheetham, J. J., R. M. Epand, M. Andrews, and T. D. Flanagan. 1990. Cholesterol sulfate inhibits the fusion of Sendai virus to biological and model membranes. *J. Biol. Chem.* 265:12404–12409.

Chen, R. F., and J. R. Knutson. 1988. Mechanism of fluorescence concentration quenching of carboxyfluorescein in liposomes: energy transfer to nonfluorescent dimers. *Anal. Biochem.* 172:61–77.

Christensen, B., J. Fink, R. B. Merrifield, and D. Mauzerall. 1988. Channel-forming properties of cecropins and related model compounds incorporated into planar lipid membranes. *Proc. Natl. Acad. Sci. USA.* 85:5072–5076.

Day, E. P., A. Y. W. Kwok, S. K. Hark, J. T. Ho, W. J. Vail, J. Bentz, and S. Nir. 1980. Reversibility of sodium-induced aggregation of sonicated phosphatidylserine vesicles. *Proc. Natl. Acad. Sci. USA.* 77:4026–4029.

Düzgünes, N., M. C. Pedroso de Lima, L. Stamatatos, D. Flasher, D. Alford, D. S. Friend, and S. Nir. 1992. Fusion activity and inactivation of influenza virus: kinetics of low pH-induced fusion with cultured cells. *J. Gen. Virol.* 73:27–37.

Düzgünes, N., and S. A. Shavnin. 1992. Membrane destabilization by N-terminal peptides of viral envelope proteins. *J. Membr. Biol.* 128: 71–80.

Epand, R. M., J. J. Cheetham, R. F. Epand, P. L. Yeagle, C. D. Richardson, A. Rockwell, and W. F. Degrado. 1992. Peptide models for the membrane destabilizing actions of viral fusion proteins. *Biopolymers.* 32: 309–314.

Fattal, E., S. Nir, R. A. Parente, and F. C. J. Szoka. 1994. pore forming peptides induce rapid phospholipid flip-flop in membranes. *Biochemistry.* 33:6721–6731.

Flory, P. J. 1939. Kinetics of polyesterification: a study of the effects of molecular weight and viscosity on reaction rate. *J. Am. Chem. Soc.* 61:3334–3340.

Frey, S., and L. K. Tamm. 1990. Membrane insertion and lateral diffusion of fluorescence-labelled cytochrome c oxidase subunit IV signal peptide in charged and uncharged phospholipid bilayers. *Biochem. J.* 272: 713–719.

Gazit, E., and Y. Shai. 1993. Structural characterization, membrane interaction, and specific assembly within phospholipid membranes of hydrophobic segments from Bacillus thuringiensis var. israelensis cytolytic toxin. *Biochemistry.* 32:12363–12371.

Ghosh, P., S. F. Mel, and R. M. Stroud. 1993. A carboxy-terminal fragment of colicin Ia forms ion channels. *J. Membr. Biol.* 134:85–92.

Harshman, S., P. Boquet, E. Duflot, J. E. Alouf, C. Montecucco, and E. Papini. 1989. Staphylococcal alpha-toxin: a study of membrane penetration and pore formation. *J. Biol. Chem.* 264:14978–14984.

Hope, M. J., M. B. Bally, G. Webb, and P. R. Cullis. 1985. Production of large unilamellar vesicles by a rapid extrusion procedure. Characterization of size distribution, trapped volume and ability to maintain a membrane potential. *Biochim. Biophys. Acta.* 812:55–65.

Lazarovici, P., C. Edwards, G. Raghunathan, and H. R. Guy. 1992. Secondary structure, permeability and molecular modeling of pardaxin pores. *J. Nat. Toxins.* 1:1–15.

Lazarovici, P., and P. I. Lelkes. 1992. Pardaxin induces exocytosis in bovine adrenal medullary chromaffin cells independent of calcium. *J. Pharmacol. Exp. Ther.* 263:1317–1326.

Lazarovici, P., N. Primor, and L. M. Loew. 1986. Purification and Pore-forming activity of two hydrophobic polypeptides from the secretion of the Red Sea Moses sole (*Pardachirus marmoratus*). *J. Biol. Chem.* 261:16704–16713.

Lear, J. D., Z. R. Wasserman, and W. F. DeGrado. 1988. Synthetic amphiphilic peptide models for protein ion channels [and erratum in *Science* 1989 245:1437]. *Science.* 240:1177–1181.

Lewis, T., and H. M. McConnel. 1978. Model lipid bilayer membranes as target for antibody-desendent, cellular- and complement-mediated immune attack. *Ann. N.Y. Acad. Sci.* 308:124–136.

Martin, I., Q. F. Defrise, V. Mandieau, N. M. Nielsen, T. Saermark, A. Burny, R. Brasseur, J. M. Ruysschaert, and M. Vandenbranden. 1991. Fusogenic activity of SIV (simian immunodeficiency virus) peptides located in the GP32 NH2 terminal domain. *Biochem. Biophys. Res. Commun.* 175:872–879.

Matsuzaki, K., M. Fukui, N. Fujii, and K. Myajima. 1993. Permeabilization and morphological changes in phosphatidylglycerol bilayers induced by an antimicrobial peptide, TachyplesrinI. *Colloid Polym. Sci.* 271: 901–908.

Merrifield, R. B., L. D. Vizioli, and H. G. Boman. 1982. Synthesis of the antibaterial peptide Cecropin A(1–33). *Biochemistry.* 21:5020–5031.

Nieva, J. L., S. Nir, A. Muga, F. M. Goni, and J. Wilschut. 1994. Interaction of the HIV-1 fusion peptide with phospholipid vesicles: different structural requirements for fusion and leakage. *Biochemistry.* 33:3201–3209.

Nir, S., J. Bentz, and A. R. J. Portis. 1980. Effect of cation concentrations and temperature on the rates of aggregation of acidic phospholipid vesicles: application to fusion. *Adv. Chem.* 188:75–106.

Nir, S., J. Bentz, J. Wilschut, and N. Duzgunes. 1983. Aggregation and fusion of phospholipid vesicles. *Prog. Surf. Sci.* 13:1–124.

Nir, S., K. Klappe, and D. Hoekstra. 1986. Kinetics and extent of fusion between Sendai virus and erythrocyte ghosts: application of a mass action kinetic model. *Biochemistry.* 25:2155–2161.

Nir, S., R. Peled, and K. Lee. 1994. Analysis of particle uptake by cells: binding to several receptors, equilibration time, endocytosis. *Colloid Surf.* 89:45–57.

Papahadjopoulos, D., K. Jacobson, S. Nir, and T. Isac. 1973. Phase transitions in phospholipid vesicles. Fluorescence polarization and permeability measurements concerning the effect of temperature and cholesterol. *Biochim. Biophys. Acta.* 311:330–348.

Parente, R. A., S. Nir, and J. Szoka F. C. 1990. Mechanism of leakage of phospholipid vesicle contents induced by the peptide GALA. *Biochemistry.* 29:8720–8728.

Peled, C. R., G. Braun, and S. Nir. 1995. Time of equilibration in reversible aggregation of particles. *J. Colloid Interface Sci.* 169:204–213.

Primor, N., J. Parness, and E. Zlotkin. 1978. Pardaxin: the toxic factor from the skin secretion of the flatfish Pardachirus marmoratus (Soleidae). *In* Toxins: Animal, Plant and Microbial. P. E. Rosenberg, editor. Pergamon Press, New York. 539.

Rafalski, M., A. Ortiz, A. Rockwell, G. L. van, J. D. Lear, W. F. DeGrado, and J. Wilschut. 1991. Membrane fusion activity of the influenza virus hemagglutinin: interaction of HA2 N-terminal peptides with phospholipid vesicles. *Biochemistry.* 30:10211–10220.

Rapaport, D., G. R. Hague, Y. Pouny, and Y. Shai. 1993. pH- and ionic strength-dependent fusion of phospholipid vesicles induced by pardaxin analogues or by mixtures of charge-reversed peptides. *Biochemistry.* 32:3291–3297.

Rapaport, D., S. Nir, and Y. Shai. 1994. Capacities of pardaxin analogues to induce fusion and leakage of negatively charged phospholipid vesicles are not necessarily correlated. *Biochemistry.* 33:12615–12624.

Rapaport, D., and Y. Shai. 1991. Interaction of fluorescently labeled pardaxin and its analogues with lipid bilayers. *J. Biol. Chem.* 266: 23769–23775.

Rapaport, D., and Y. Shai. 1992. Aggregation and organization of pardaxin in phospholipid membranes. A fluorescence energy transfer study. *J. Biol. Chem.* 267:6502–6509.

Rouser, B., A. Siakotos, and S. Fleischer. 1966. Quantitative analysis of phospholipid by thin layer chromatography and phosphorous analysis of spots. *Lipids.* 1:85–86.

Schwarz, G., and G. Beschiaschvili. 1989. Thermodynamic and kinetic studies on the association of melittin with a phospholipid bilayer. *Biochim. Biophys. Acta.* 979:82–90.

Schwarz, G., S. Stankowski, and V. Rizzo. 1986. Thermodynamic analysis of incorporation and aggregation in a membrane: application to the pore-forming peptide alamethicin. *Biochim. Biophys. Acta.* 861: 141–151.

Shai, Y. 1994. Pardaxin: channel formation by a shark repellant peptide from fish. *Toxicology.* 87:109–129.

Shai, Y., D. Bach, and A. Yanovsky. 1990. Channel formation properties of synthetic pardaxin and analogues. *J. Biol. Chem.* 265:20202–20209.

Shai, Y., J. Fox, C. Caratsch, Y. L. Shih, C. Edwards, and P. Lazarovici. 1988. Sequencing and synthesis of pardaxin, a polypeptide from the Red Sea Moses sole with ionophore activity. *FEBS. Lett.* 242:161–166.

Shai, Y., Y. R. Hadari, and A. Finkels. 1991. pH-dependent pore formation properties of pardaxin analogues. *J. Biol. Chem.* 266:22346–22354.

Smoluchowski, M. V. 1917. Versuch einer mathematischen Theorie der Koagulationskinetik Koloider Losungen. *Z. Phys. Chem. Stochiometrie Vervandschaftsl.* 92:129–168.

Spruce, A. E., A. Iwata, J. M. White, and W. Almers. 1989. Patch clamp studies of single cell-fusion events mediated by a viral fusion protein. *Nature.* 342:555–558.

Steiner, H., D. Andreu, and R. B. Merrifield. 1988. Binding and action of cecropin and cecropin analogues: antibacterial peptides from insects. *Biochim. Biophys. Acta.* 939:260–266.

Struck, K. D., D. Hoekstra, and R. E. Pagano. 1981. Use of resonance energy transfer to monitor membrane fusion. *Biochemistry.* 20: 4093–4099.

Szoka, F. C., and D. Papahadjopoulos. 1980. Comparative properties and methods of preparation of lipid vesicles (liposomes). *Annu. Rev. Biophys. Bioeng.* 9:467–508.

Weinstein, J. N., R. D. Klausner, T. Innerarity, E. Ralston, and R. Blumenthal. 1981. Phase transition release, a new approach to the interaction of proteins with lipid vesicles. Application to lipoproteins. *Biochim. Biophys. Acta.* 647:270–284.

White, J. M. 1992. Membrane fusion. *Science.* 258:917–924.

Wu, D., and A. I. Aronson. 1992. Localized mutagenesis defines regions of the Bacillus thuringiensis delta-endotoxin involved in toxicity and specificity. *J. Biol. Chem.* 267:2311–2317.

Zasloff, M. 1992. Antibiotic peptides as mediators of innate immunity. *Curr. Opin. Immunol.* 4:3–7.